Optica Applicata, Vol. L, No. 2, 2020
DOI: 10.37190/oa200203

Single air-mode resonance photonic crystal nanofiber cavity for ultra-high sensitivity refractive index sensing

YANNI ZHANG[1], JIAXI YANG[1], MEIQI SONG[1], XUAN ZHANG[2], DAQUAN YANG[2*]

[1]International School, Beijing University of Posts and Telecommunications, Beijing 100876, China

[2]School of Information and Communication Engineering,
Beijing University of Posts and Telecommunications, Beijing 100876, China

[*]Corresponding author: ydq@bupt.edu.cn

We propose a design of series-connected one-dimensional photonic crystal nanofiber cavity sensor (1-D PC-NCS) and one-dimensional photonic crystal nanofiber bandgap filter (1-D PC-NBF). The proposed structure can get a single air mode for refractive index sensing with its extinction ratio of 58.64 dB. It filters out the high order mode and reduces the interaction between signals. By 3D FDTD, the calculated sensitivity is 848.18 nm/RIU (RIU – refractive index unit). Compared with general silicon on-chip nanobeam cavity, the sensitivity is increased by eight times. The additional 1-D PC-NBF will not change the sensitivity and the position of the resonance wavelength. Therefore, the new design we propose addresses the issue of crosstalk, and can be applied to ultra -high sensitivity index-based gas sensing and biosensing without the need for complicated coupling systems.

Keywords: photonic crystal nanocavity, air mode nanofiber, refractive index sensor, sensitivity.

1. Introduction

In recent years, optical sensors based on micro/nanofiber cavity have excellent performance in sensing applications [1, 2]. The remarkable optical and mechanical properties exhibited by micro/nanofiber cavity include large evanescent fields, strong light confinement and ultra-high transmission [3]. Such desirable characteristics have gathered much attention in decades. HILL *et al.* has fabricated refractive index Bragg gratings in photosensitive optical fiber by using a special phase mask grating made of silica glass [4]. ZHI-YUAN LI has theoretically designed and experimentally realized a broadband ultrasmall microcavity for sensing a varying number of microparticles in a freely suspended microfiber [5]. So far, the compact form of nanofiber microcavities based optical sensors makes sensing refractive index in microfluidic channels and humidity environments highly feasible and robust [6–10].

However, although the optical nanofiber-based microcavities mentioned above have shown extraordinary performance in some specific fields, they also have some shortcomings. For example, the length of a traditional fiber Bragg grating usually consists of hundreds of periods, indicating a large mode volume [4, 11]. To solve that problem, YANG *et al.* proposed the design of low-index-contrast photonic crystal nanofiber cavity for high sensitive refractive index sensing, which can achieve small mode volume [3]. Though the sensitivity of that design is 736.80 nm/RIU (RIU – refractive index unit), when multiplexing, crosstalk happens. That makes it difficult to distinguish the target resonance peak from the jamming signals.

To tackle the crosstalk problem, a filter needs to be introduced. Therefore, we propose a 1-D PC nanofiber sensor device for high sensitivity refractive index sensing in this paper. The design connects one-dimensional photonic crystal nanofiber bandgap filter (1-D PC-NBF) and one-dimensional photonic crystal nanofiber cavity sensor (1-D PC-NCS) in series so that the single air mode with the extinction ratio of 58.64 dB can be obtained, which addresses the issue of crosstalk mentioned above. It is worth mentioning that the sensitivity of design can reach up to 848.18 nm/RIU which is extremely high in comparison with general silicon on-chip nanobeam cavity sensor [12].

The organization of this paper is as follows. In Section 2, the design concept and realization of the integrated 1-D PC nanofiber sensor device are discussed. In Section 3, the parameters and characteristics of the integrated 1-D PC nanofiber sensor device is introduced in detail. Finally, in Section 4, we draw a brief conclusion.

2. The design of 1-D PC-NCS series-connected 1-D PC-NBF with single air mode

The integrated 1-D PC nanofiber sensor device we propose consists of two parts, as shown in Fig. 1.

The first part is 1-D PC-NCS with a high-sensitivity (S = 847.77 nm/RIU). The periodicity is α_1 = 629 nm, and the radii of air-hole gratings increase quadratically from r_{center} = 195 nm to r_{end} = 240 nm which follows the formula

$$r(i) = r_{\text{center}} + (i-1)^2 \frac{r_{\text{end}} - r_{\text{center}}}{(i_{\max} - 1)^2} \tag{1}$$

where i increases from 1 to $i_{\max}$; $i_{\max}$ is the grating number in the Gaussian mirror taper region of 1-D PC-NCS [13]. Here we choose $i_{\max}$ = 36 for better simulation results.

The second part is 1-D PC-NBF. The periodicity is α_2 = 629 nm, and the radii of air-hole gratings keep the same as r_1 = 300 nm.

Figure 2**a** displays the composed transmission spectrum as a function of increased refractive index (RI) changed from RI = 1.00 to RI = 1.10. It has high sensitivity (S = 847.77 nm/RIU) as shown in Figure 2**b**. However, if multiple cavity sensors are

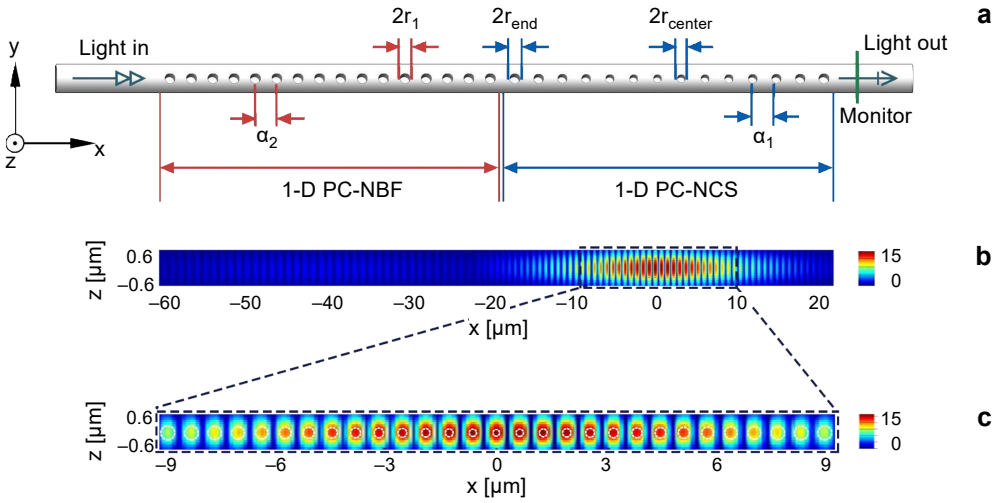

Fig. 1. Structure diagram of the integrated 1-D PC nanofiber sensor device, which consists of 1-D PC-NCS and 1-D PC-NBF. The period is $\alpha_1 = \alpha_2 = 629$ nm. For 1-D PC-NCS, the radii of air-hole gratings increase quadratically from $r_{center} = 195$ nm to $r_{end} = 240$ nm. For 1-D PC-NBF, the radii of air-hole gratings keep the same as $r_1 = 300$ nm (**a**). The major electric field distribution in y direction ($|E_y|$) of the fundamental resonant mode in the integrated 1-D PC nanofiber sensor (by 3D FDTD) (**b**). Enlarged drawing of the major electric field distribution corresponding to part **b** (**c**).

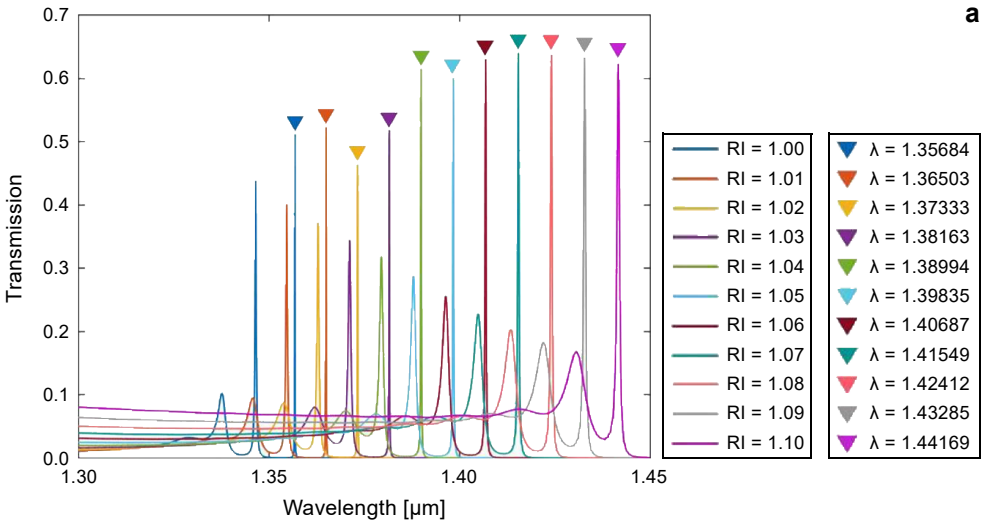

Fig. 2. The relation between resonant wavelength and refractive index (RI) in the 1-D PC nanofiber sensor without filter. The resonant wavelength shifts along with the RI increased from 1.00 to 1.10 (**a**). The relation between resonant wavelength and RI in the single 1-D PC-NCS (without 1-D PC-NBF). The sensitivity of the sensor is 847.77 nm/RIU (**b**). The marked resonant wavelength in part **a** corresponds to the data point in part **b**.

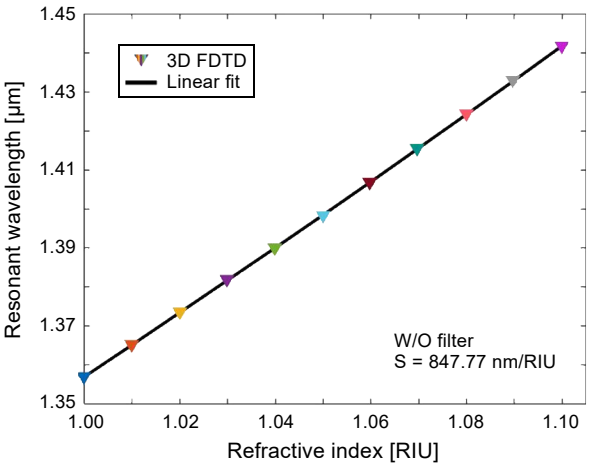

Fig. 2. Continued.

series-connected, the output transmission signals from different cavity sensors will be combined at the output, resulting in the issue of the mixing of high order resonance with fundamental mode. More specifically, when $\lambda = 1356.84$ nm, the high mode when RI = 1.01 (the orange line) may interfere with the fundamental mode when RI = 1.00 (the blue line).

This phenomenon can be exceedingly troublesome to 1-D PC-NCS. It makes 1-D PC-NCS difficult to be used for multiplexed sensing because the sensing signal of every sensor may interact with each other. In addition, it also hampers 1-D PC-NCS achieving smart screening detection because it may easily cause researchers choosing wrong resonant mode (*e.g.* other high order modes) rather than the preset fundamental mode for multiplexed sensing detection during the practical detection process [12]. To solve this problem, we construct a filter to filter out the high order mode.

We design the filter based on the characteristic of a photonic bandgap (PBG) which is the grey area between the upper and nether line as shown in Fig. 3**a**. PBG can block the light at specific wavelength or wave band. In other words, the resonant wavelength lying in the PBG region of 1-D PC-NBF cannot be guided. Therefore, the characteristics of PBG makes it possible for us to achieve the purpose of filtering and thus enables us to get the fundamental mode as a sensing signal.

Numerical simulations have demonstrated that as the effective refractive index increased (*e.g.* by reducing air-hole grating radius), the photonics bandgap (PBG) of the structure moves to lower frequency [14]. Therefore, with proper engineering of the structure parameters of 1-D PC-NBF, an arbitrary wavelength range bandgap can be obtained.

The goal is filtering out air modes 2 and 3 (AM2 and AM3). After doing numerical simulations, we realize that the filter with air hole radii $r = 300$ nm has the best filtering performance for the purposed sensor structure with a high pass bandgap ranging from 1284.9 to 1345.9 nm. By using 3D FDTD, we get the TE band diagram of the unit cell

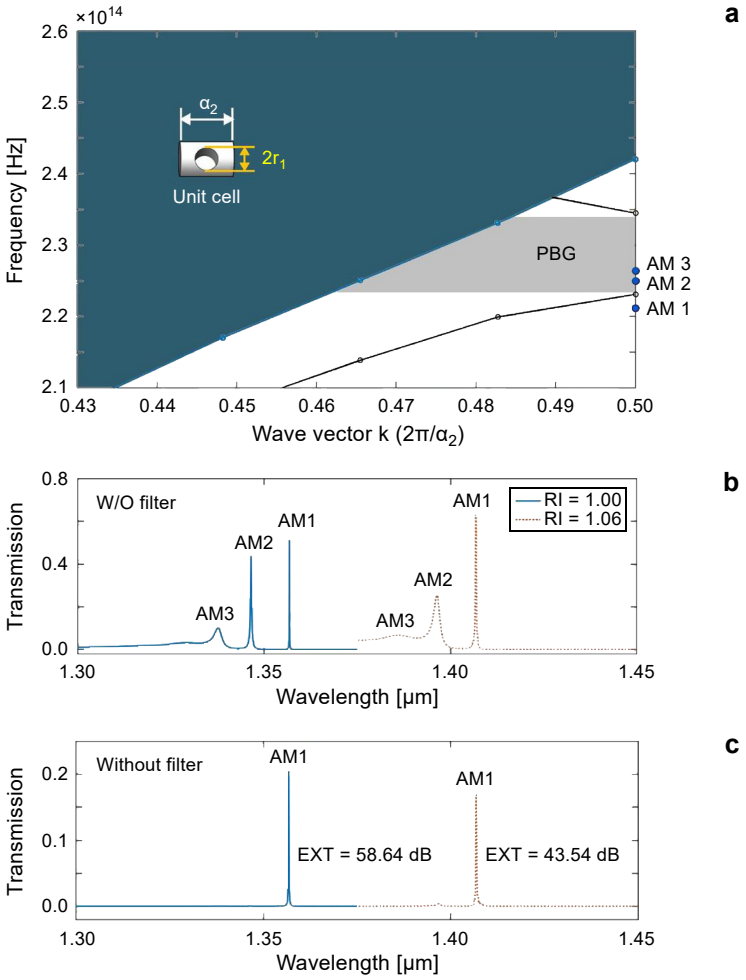

Fig. 3. TE band diagram of 1-D PC-NBF with air-hole radii r_1 = 300 nm and period α_2 = 629 nm. On the right border of this diagram, three blue points correspond to air mode AM1, AM2 and AM3 when RI = 1.00 in part **b** (**a**). Transmission spectrum of the single 1-D PC-NCS (without filter) when RI = 1.00 and RI = 1.06. Here, AM1 is the fundamental mode and AM2, AM3 are the high order mode (**b**). Transmission spectrum of the integrated 1-D PC nanofiber sensor device we propose whose EXT = 58.64 dB (RI = 1.00), and EXT = 43.54 dB (RI = 1.06) (**c**).

with air-hole radii r = 300 nm, period α_2 = 629 nm as shown in Fig. 3**a**. We can see there are three points marked on the right border of Fig. 3**a**. The points marked AM2 and AM3 in Fig. 3**b** lie in PBG and cannot be transmitted through the filter. And the point marked AM1 lies outside the PBG. As a result, after integrated with 1-D PC-NBF, only AM1 will remain. In other words, we obtain single air mode (Fig. 3**c**). It indicates that the proposed device eliminates AM2 and AM3 successfully.

Furthermore, the position of the resonance wavelength does not change. Figure 3**b** shows the transmission spectrum of a single 1-D PC-NCS when RI = 1.00 (blue line)

and RI = 1.06 (orange line). It turns out that the additional series connected 1-D PC filter has no influence on the resonant wavelength of the fundamental mode and can attain extinction ratio (EXT) of 58.64 and 43.54 dB when RI = 1.00 and RI = 1.06 correspondingly, as shown in Fig. 3**c**.

Therefore, the integrated sensor device proposed in this paper can be the basis for building the nanofiber densely integrated sensors array, which can be used for accurate sensing with high parallel multiplexing capability [15].

3. Single resonance nanofiber cavity sensor characteristics

Figure 4 shows the proposed integrated 1-D PC nanofiber sensor device, with 1-D PC-NCS series-connected 1-D PC-NBF. In the integrated 1-D PC nanofiber sensor device, light incidents from the left side of the device, couples with the cavities in the intermediate section. Then we are able to realize the purpose of sensing through observing the shift of the resonant peak.

The structure of the sensor is centrosymmetric. The cavities are etched into a SiO_2 fiber (n_{SiO_2} = 1.45, r = 520 nm). The radii of sensors cavities are increased from the

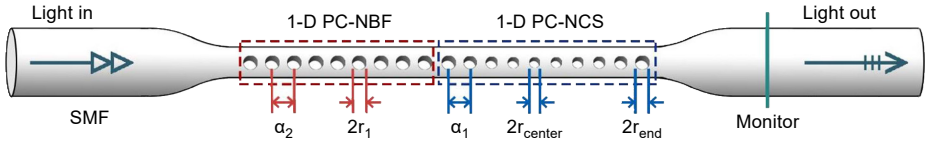

Fig. 4. Schematic illustration of the integrated 1-D PC nanofiber sensor device, which consists of 1-D PC-NCS and 1-D PC-NBF. The period is $\alpha_1 = \alpha_2 = 629$ nm. For 1-D PC-NCS, the radii of air-hole gratings increase quadratically from $r_{center} = 195$ nm to $r_{end} = 240$ nm. For 1-D PC-NBF, the radii of air-hole gratings keep the same as $r_1 = 300$ nm.

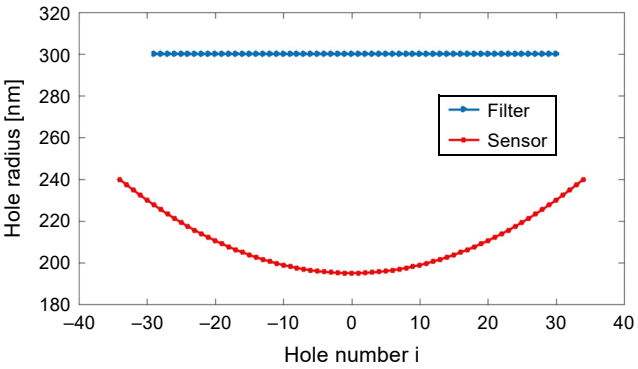

Fig. 5. Schematic diagram of relation between hole radius and the hole number of 1-D PC-NCS and 1-D PC-NBF. The blue straight line represents the relation between the hole radius and the hole number of 1-D PC-NBF. There are 60 points in the blue straight line, which means there are 60 holes on the filter and these holes radii are the same. The red curve represents the relation between the hole radius and the hole number of 1-D PC-NCS. There are 71 points in the red curve which means there are 71 holes on the sensor. The changing trend of the radius is quadratic.

center to the end, which follow the Eq. (1) where $r_{end} = 240$ nm, $r_{center} = 195$ nm. Since we choose the air mode for the sensor, the symcenter of the sensor should be an air cavity. It should be noted that though $i_{max} = 36$, due to the formula mentioned above, in fact there are 71 cavities drilled into the fiber.

The filter's structure is also centrosymmetric, where the radii of air-hole gratings are kept same as $r_1 = 300$ nm and the total number of the cavities is 60. The specific relation between the hole radius and the hole number is shown in Fig. 5.

Figure 6**a** shows the composed transmission spectra of the proposed integrated 1-D PC nanofiber sensor device which is formed by series-connected 1-D PC-NBF and

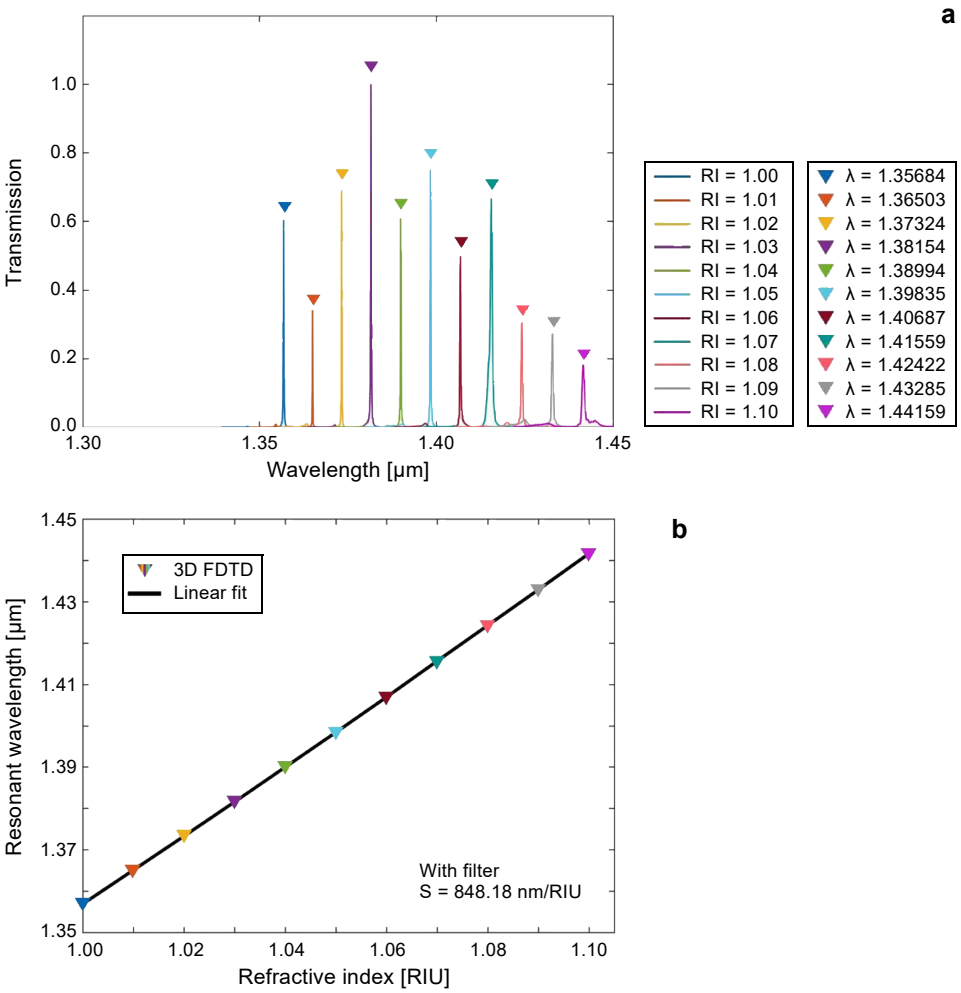

Fig. 6. The relation between the resonant wavelength and the refractive index (RI) in the integrated 1-D PC nanofiber sensor device (**a**). The relation between the resonant wavelength and the refractive index in the single integrated 1-D PC nanofiber sensor device (**b**). By 3D FDTD, we can calculate the sensitivity (848.18 nm/RIU) of the sensor device. The marked resonant wavelength in part **a** corresponds to the data point in part **b**.

1-D PC-NCS when the refractive index changes from RI = 1.00 to RI = 1.10. As we can see, the issue of the interaction between the high order resonant mode and the fundamental mode can be well addressed.

The sensitivity of this new resonance nanofiber cavity sensor we proposed keeps consistent with that of the optical sensor without filter. More specifically, the sensitivity of the sensor is 847.77 nm/RIU while the sensitivity of the sensor in series with filter is 848.18 nm/RIU (Fig. 6**b**). That indicates the filter has no interference on the sensitivity. Compared with the general silicon on-chip nanobeam sensors, the sensitivity of the nanofiber cavity sensor is increased by eight times [16–18].

4. Conclusion

In summary, we propose a design of 1-D PC nanofiber sensor device with series-connected 1-D PC-NBF and 1-D PC-NCS by 3D FDTD. It can address the issue of the interaction between signals due to crosstalk. We attain a photonic bandgap (PBG) that filters out the jamming signal and consequently makes the proposed structure become a filter with excellent performance. Then, by connecting 1-D PC-NBF and 1-D PC-NCS in series, a transmission only containing a single air mode for sensing detection can be obtained. The design enables us to filter out the high order mode and get the single air mode for sensing. Besides, the additional 1-D PC-NBF has no influence on resonance wavelength which means the position of the resonance wavelength does not change. It is worth mentioning that the sensitivity of the new resonance nanofiber cavity sensor is ultra-high and keeps consistent with that of a single optical sensor. The design presented here has the potential to make huge contribution to ultra-compact integrated sensor-array devices and accelerate the development of other photonic integrated devices.

Acknowledgements – This work was supported by the National Natural Science Foundation of China (NSFC) (11974058); Fundamental Research Funds for the Central Universities (2018XKJC05); China Postdoctoral Science Foundation (2018M640015); and Fund of the State Key Laboratory of Information Photonics and Optical Communications (IPOC2019ZT03), BUPT, China.

References

[1] FAN X., WHITE I.M., SHOPOVA S.I., ZHU H., SUTER J.D., SUN Y., *Sensitive optical biosensors for unlabeled targets: a review*, Analytica Chimica Acta **620**(1–2), 2008, pp. 8–26, DOI: 10.1016/j.aca.2008.05.022.

[2] CHEN G.Y., DING M., NEWSON T.P., BRAMBILLA G., *A review of microfiber and nanofiber based optical sensors*, Open Optics Journal **7**(1), 2013, pp. 32–57, DOI: 10.2174/1874328501307010032.

[3] YANG D., CHEN X., ZHANG X., LAN C., ZHANG Y., *High-Q, low-index-contrast photonic crystal nanofiber cavity for high sensitivity refractive index sensing*, Applied Optics **57**(24), 2018, pp. 6958–6965, DOI: 10.1364/AO.57.006958.

[4] HILL K.O., MALO B., BILODEAU F., JOHNSON D.C., ALBERT J., *Bragg gratings fabricated in monomode photosensitive optical fiber by UV exposure through a phase mask*, Applied Physics Letters **62**(10), 1993, pp. 1035–1037, DOI: 10.1063/1.108786.

[5] Yu Y., Xiao T.-H., Guo H.-L., Li Z.-Y., *Sensing of microparticles based on a broadband ultrasmall microcavity in a freely suspended microfiber*, Photonics Research **5**(3), 2017, pp. 143–150, DOI: 10.1364/PRJ.5.000143.

[6] Polynkin P., Polynkin A., Peyghambarian N., Mansuripur M., *Evanescent field-based optical fiber sensing device for measuring the refractive index of liquids in microfluidic channels*, Optics Letters **30**(11), 2005, pp. 1273–1275, DOI: 10.1364/OL.30.001273.

[7] Kude V.P., Khairnar R.S., *Fabrication and numerical evaluation of the tapered single mode optical fiber: detection of change in refractive index*, Indian Journal of Pure and Applied Physics **46**(1), 2008, pp. 23–29.

[8] Sui C., Wu P., Ye B., *Highly sensitive sensor for detecting refractive index change of liquids using single microfiber*, [In] *2010 3rd International Nanoelectronics Conference (INEC)*, 2010, pp. 1343–1344, DOI: 10.1109/INEC.2010.5424870.

[9] Wang P., Brambilla G., Ding M., Semenova Y., Wu Q., Farrell G., *High-sensitivity, evanescent field refractometric sensor based on a tapered, multimode fiber interference*, Optics Letters **36**(12), 2011, pp. 2233–2235, DOI: 10.1364/OL.36.002233.

[10] Biazoli C.R., Silva S., Franco M.A.R., Frazão O., Cordeiro C.M.B., *Multimode interference tapered fiber refractive index sensors*, Applied Optics **51**(24), 2012, pp. 5941–5945, DOI: 10.1364/AO.51.005941.

[11] Hill K.O., Meltz G., *Fiber Bragg grating technology fundamentals and overview*, Journal of Lightwave Technology **15**(8), 1997, pp. 1263–1276, DOI: 10.1109/50.618320.

[12] Yang D., Tian H., Ji Y., Quan Q., *Design of simultaneous high-Q and highsensitivity photonic crystal refractive index sensors*, Journal of the Optical Society of America B **30**(8), 2013, pp. 2027–2031, DOI: 10.1364/JOSAB.30.002027.

[13] Zhi Y., Yu X.-C., Gong Q., Yang L., Xiao Y.-F., *Single nanoparticle detection using optical microcavities*, Advanced Materials **29**(12), 2017, article 1604920, DOI: 10.1002/adma.201604920.

[14] Liang F., Guo Y., Hou S., Quan Q., *Photonic-plasmonic hybrid singlemolecule nanosensor measures the effect of fluorescent labels on DNA-protein dynamics*, Science Advances **3**(5), 2017, article e1602991, DOI: 10.1126/sciadv.1602991.

[15] Zhang Y., Liu P., Zhang S., Liu W., Chen J., Shi Y., *High sensitivity temperature sensor based on cascaded silicon photonic crystal nanobeam cavities*, Optics Express **24**(20), 2016, pp. 23037–23043, DOI: 10.1364/OE.24.023037.

[16] Quan Q., Floyd D.L., Burgess I.B., Deotare P.B., Frank I.W., Tang S.K.Y., Ilic R., Loncar M., *Single particle detection in CMOS compatible photonic crystal nanobeam cavities*, Optics Express **21**(26), 2013, pp. 32225–32233, DOI: 10.1364/OE.21.032225.

[17] Liang F., Clarke N., Patel P., Loncar M., Quan Q., *Scalable photonic crystal chips for high sensitivity protein detection*, Optics Express **21**(26), 2013, pp. 32306–32312, DOI: 10.1364/OE.21.032306.

[18] Quan Q., Loncar M., *Deterministic design of wavelength scale, ultra-high Q photonic crystal nanobeam cavities*, Optics Express **19**(19), 2011, pp. 18529–18542, DOI: 10.1364/OE.19.018529.

Received March 21, 2019
in revised form June 8, 2019